Numerical Analysis of Damage and Failure in Anisotropic Sheet Metals During Biaxial Loading

Michael Brünig, Sanjeev Koirala, and Steffen Gerke

Abstract In the paper, the influence of stress state and loading direction with respect to the principal axes of anisotropy on damage and fracture behavior of the anisotropic aluminum alloy EN AW-2017A is discussed. The focus is on numerical calculations on the micro-level considering void-containing representative volume elements revealing information on damage mechanisms. Using experimental data taken from uniaxial and biaxial tests, material parameters are identified. Based on numerical studies on the micro-scale with differently loaded void-containing cubes, it is shown that the stress state, the load ratio and the loading direction with respect to the principal axes of anisotropy have an influence on evolution of damage processes on the micro-scale and on the corresponding damage strains.

Keywords Ductile damage · Anisotropic metals · Micro-mechanical studies

1 Introduction

Numerical analysis of deformation and failure behavior of complex structures requires accurate modeling of inelastic behavior of materials. In this context, various constitutive theories and corresponding robust and efficient numerical techniques have been discussed during the last decades. For example, failure in ductile metals is mainly caused by nucleation, growth and coalescence of micro-defects leading to the evolution of macro-cracks. Therefore, a straight-forward way for the formulation of appropriate constitutive models should be based on the analysis of the behavior of individual micro-defects in elastic-plastic materials [5, 7]. The results of these calculations on the micro-scale can then be used to develop macroscopic phenomenological approaches which, for example, can be used to analyze the deformation and failure behavior of ductile metals during forming operations.

M. Brünig (✉) · S. Koirala · S. Gerke
Institut für Mechanik und Statik, Universität der Bundeswehr München, 85577 Neubiberg, Germany
e-mail: michael.bruenig@unibw.de

J. Kusiak et al. (eds.), *Numerical Methods in Industrial Forming Processes*, Lecture Notes in Mechanical Engineering, https://doi.org/10.1007/978-3-031-58006-2_22

To get insight into damage and failure mechanisms in ductile metals and to examine the behavior of micro-defects caused by various loading conditions, three-dimensional finite element simulations of microscopic cell models have been performed by different research groups; see, for example, [1, 5, 10, 11, 16–18]. These investigations based on the assumption of isotropic elastic-plastic material behavior showed that the current stress state remarkably affects the damage and failure processes on the micro-level as well as the corresponding macroscopic behavior. The numerical results of the unit cell calculations can be used to propose and validate damage evolution equations in phenomenological continuum models and to determine micro-mechanically motivated constitutive parameters [5, 7].

Manufacturing processes such as rolling, deep drawing or extrusion cause anisotropies in ductile metals resulting from internal changes in the crystallographic structure. These deformation-induced anisotropies must be taken into consideration in material models used to simulate the deformation and failure behavior of thin metal sheets. Different anisotropic yield criteria for hydrostatic-stress-independent material behavior have been presented in the literature based on quadratic [13, 19], non-quadratic [2, 12, 15] or spline functions [20]. In addition, the Hoffman yield condition [14] has been developed to take into account the strength-differential effect in anisotropic materials.

In the present paper, micro-mechanical numerical simulations with spherical void-containing representative volume elements are discussed. The plastic anisotropy of the investigated ductile metal is modeled by the Hoffman yield criterion. Different load combinations are taken into account with respect to the principal axes of anisotropy. Numerical results of these micro-mechanical calculations are used to reveal the effect of stress state, of load ratio and of loading direction on damage mechanisms as well as on corresponding damage strains.

2 Constitutive Model

The numerical analysis is based on the continuum damage model presented by [3–5] which has been enhanced for anisotropic plasticity by [6, 8, 9]. The framework uses the introduction of the damage strain tensor, $\mathbf{A}^{da}$, characterizing the formation of macroscopic strains caused by damage processes on the micro-scale. In addition, the kinematics take into account the additive decomposition of the strain rate tensor into elastic, $\dot{\mathbf{H}}^{el}$, effective plastic, $\dot{\bar{\mathbf{H}}}^{pl}$, and damage parts, $\dot{\mathbf{H}}^{da}$ [3].

Anisotropic plastic behavior of the investigated aluminum alloy EN AW-2017A is modeled by the Hoffman yield condition [14]

$$f^{pl} = \mathbf{C} \cdot \bar{\mathbf{T}} + \sqrt{\frac{1}{2}\bar{\mathbf{T}} \cdot \mathcal{D}\,\bar{\mathbf{T}}} - c = 0, \tag{1}$$

where $\bar{\mathbf{T}}$ denotes the effective Kirchhoff stress tensor defined in the fictitious undamaged configuration and the tensor of coefficients

$$\mathbf{C} = C^i_{.j}\, \mathbf{g}_i \otimes \mathbf{g}^j = C_{(i)}\, \mathbf{g}_i \otimes \mathbf{g}^i \tag{2}$$

with the components (in Voigt notation)

$$\left[C^i_{.j}\right] = [C_1 \;\; C_2 \;\; C_3 \;\; 0 \;\; 0 \;\; 0]^T \tag{3}$$

has been used. In addition, further material parameters describing the plastic anisotropy are given by the tensor

$$\mathcal{D} = D^{i.k}_{.j.l}\, \mathbf{g}_i \otimes \mathbf{g}^j \otimes \mathbf{g}_k \otimes \mathbf{g}^l \tag{4}$$

with

$$\left[D^{i.k}_{.j.l}\right] = \begin{bmatrix} C_4 + C_5 & -C_4 & -C_5 & 0 & 0 & 0 \\ -C_4 & C_4 + C_6 & -C_6 & 0 & 0 & 0 \\ -C_5 & -C_6 & C_5 + C_6 & 0 & 0 & 0 \\ 0 & 0 & 0 & C_7 & 0 & 0 \\ 0 & 0 & 0 & 0 & C_8 & 0 \\ 0 & 0 & 0 & 0 & 0 & C_9 \end{bmatrix} \tag{5}$$

and

$$c = c_o + R_o \epsilon^{pl} + R_\infty \left(1 - e^{-b\,\epsilon^{pl}}\right) \tag{6}$$

represents the equivalent yield stress of the undamaged metal. For the investigated ductile anisotropic aluminum alloy EN AW-2017A the parameters are listed in Table 1.

They have been identified by a uniaxial tension test of a flat specimen cut in the rolling direction of the aluminum alloy sheet. The anisotropy parameters C_i in Eqs. (3) and (5) are determined considering the stress-strain behavior of uniaxially loaded specimens cut in different directions with respect to the rolling direction [9]. These parameters are listed in Table 2.

Based on the yield criterion (1) generalized invariants of the effective Kirchhoff stress tensor $\bar{\mathbf{T}}$ are defined [9]: the first Hoffman stress invariant is given by

$$\bar{I}_1^H = \frac{1}{a}\mathbf{C} \cdot \bar{\mathbf{T}} \quad \text{with} \quad a = \frac{1}{3}\,\text{tr}\mathbf{C} \tag{7}$$

Table 1 Plastic material parameters

	c_o [MPa]	R_o [MPa]	R_∞ [MPa]	b
RD	333	488	142	19

Table 2 Anisotropy parameters

C_1	C_2	C_3	C_4	C_5	C_6	C_7	C_8	C_9
–0.0424	–0.0102	0.0000	0.8123	1.3607	1.3103	3.7580	3.0000	3.0000

whereas the second and third deviatoric stress invariants are defined as

$$\bar{J}_2^H = \frac{1}{2}\bar{\mathbf{T}} \cdot \mathcal{D}\,\bar{\mathbf{T}} \tag{8}$$

and

$$\bar{J}_3^H = \det\left(\mathcal{D}\,\bar{\mathbf{T}}\right). \tag{9}$$

Based on these definitions the generalized Hoffman stress triaxiality

$$\bar{\eta}^H = \frac{\bar{I}_1^H}{3\sqrt{3\bar{J}_2^H}} \tag{10}$$

and the generalized Hoffman Lode parameter

$$\bar{L}^H = \frac{-3\sqrt{3}\,\bar{J}_3^H}{2\,(\bar{J}_2^H)^{(3/2)}} \tag{11}$$

are defined to characterize the dependence of anisotropic metals on the current stress state. Formation of plastic strains is governed by the flow rule

$$\dot{\bar{\mathbf{H}}}^{pl} = \dot{\gamma}\bar{\mathbf{N}} \tag{12}$$

with the equivalent plastic strain rate $\dot{\gamma}$ and the normalized deviatoric effective stress tensor

$$\bar{\mathbf{N}} = \frac{\mathcal{D}\,\bar{\mathbf{T}}}{\left\|\mathcal{D}\,\bar{\mathbf{T}}\right\|}. \tag{13}$$

Furthermore, the onset and evolution of damage in plastically anisotropic ductile materials are modeled by the damage criterion

$$f^{da} = \alpha I_1^H + \beta\sqrt{J_2^H} - \sigma = 0 \tag{14}$$

where I_1^H and J_2^H are the generalized first and second deviatoric Hoffman invariants of the Kirchhoff stress tensor formulated with respect to the damaged configurations, and σ is the equivalent damage stress measure. The parameters α and β depend on stress state and loading direction and have been identified by a series of experiments

performed with different biaxially loaded specimens; see [9] for further details. In addition, the evolution of macroscopic irreversible strains caused by damage mechanisms on the micro-level is characterized by the damage rule

$$\dot{\mathbf{H}}^{da} = \dot{\mu}\left(\frac{1}{\sqrt{3}}\tilde{\alpha}\mathbf{1} + \tilde{\beta}\mathbf{N}\right) \tag{15}$$

where

$$\mathbf{N} = \frac{\mathrm{dev}\mathbf{T}}{\|\mathrm{dev}\mathbf{T}\|} \tag{16}$$

is the normalized deviatoric part of the Kirchhoff stress tensor and the parameters $\tilde{\alpha}$ and $\tilde{\beta}$ represent the stress and loading direction dependence of the damage strain rate tensor (15).

3 Numerical Analysis

In the proposed continuum framework, the formation of damage is characterized by the evolution of macroscopic damage strains corresponding to different damage and failure processes on the micro-level. To detect the stress state and loading direction dependence of the parameters $\tilde{\alpha}$ and $\tilde{\beta}$ in the damage rule (15), numerical simulations with a void-containing representative volume element with initial porosity of 3% have been performed undergoing various three-dimensional loading conditions. One eighth of the unit cell model is shown in Fig. 1. The numerical simulations are performed using the finite element program ANSYS enhanced by a user-defined subroutine taking into account the proposed anisotropic continuum model. Eight-node elements of type SOLID185 are used. With symmetry boundary conditions the unit cell can be seen as a part of a pre-damaged structural element. The solid elements are elastically and plastically deformed whereas the changes in size and shape of the initially spherical void are related to the damage strains. Based on the proposed kinematic approach the components of the macroscopic strain rate tensor in the principal directions (i) are decomposed

$$\dot{H}_{(i)}^{\text{unit-cell}} = \dot{H}_{(i)}^{el} + \dot{H}_{(i)}^{pl} + \dot{H}_{(i)}^{da} \tag{17}$$

into elastic, plastic and damage strain rates. Elastic and plastic strain rates in the solid elements on the micro-level, $\dot{\mathbf{h}}^{el}$ and $\dot{\mathbf{h}}^{pl}$, lead to the elastic-plastic macroscopic strain rates

$$\dot{\mathbf{H}}^{ep} = \dot{\mathbf{H}}^{el} + \dot{\mathbf{H}}^{pl} = \frac{1}{V}\int_{V_{\text{matrix}}} \left(\dot{\mathbf{h}}^{el} + \dot{\mathbf{h}}^{pl}\right) dv \tag{18}$$

where V represents the current volume of the representative volume element and V_{matrix} is the current volume of the matrix material (solid elements). With Eqs. (17) and (18) the macroscopic damage strain rate tensor can be written in the form

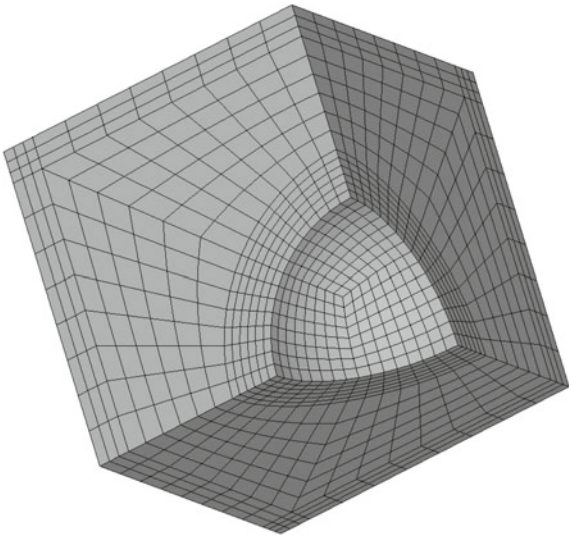

Fig. 1 Finite element mesh of one eighth of the unit cell

$$\dot{H}_{(i)}^{da} = \dot{H}_{(i)}^{\text{unit-cell}} - \dot{H}_{(i)}^{ep} \tag{19}$$

leading to the principal components of the damage strain tensor

$$A_{(i)}^{da} = \int \dot{H}_{(i)}^{da} \mathrm{d}t. \tag{20}$$

In addition, the void volume fraction f of the unit cell is determined using the volumetric part of the damage strain rate tensor leading to

$$\dot{f} = (1 - f)\,\mathrm{tr}\dot{\mathbf{H}}^{da} \tag{21}$$

and

$$f = \int \dot{f} \mathrm{d}t, \tag{22}$$

see [3] for further details. In the numerical analysis, the amount of strains and their rates are taken to be described by corresponding scalar-valued measures, the equivalent strain rate

$$\dot{\epsilon}_{eq} = \sqrt{\frac{2}{3}\dot{\mathbf{H}} \cdot \dot{\mathbf{H}}} \tag{23}$$

and the equivalent strain

$$\epsilon_{eq} = \int \dot{\epsilon}_{eq} \mathrm{d}t. \tag{24}$$

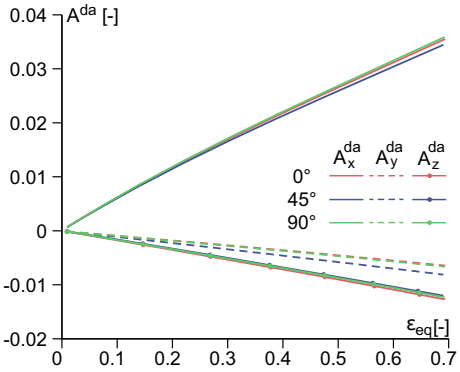

Fig. 2 Formation of principal components of the damage strain tensor for $\eta^H = 0.389$ and $L^H = -0.731$

4 Numerical Results

The effect of different load ratios $F_x/F_y/F_z$ on the damage behavior of the unit cell has been examined. In the present paper, two cases are discussed. The numerical results are compared with experimental observations reported in the literature. For example, in [6] the X0-specimen had been biaxially loaded with the load ratios $F_1/F_2 = 1/0$ and 1/–1 leading to tensile and shear dominated stress states, respectively.

For the load ratio $F_1/F_2 = 1/0$, the Hoffman stress triaxiality $\eta^H = 0.389$ and the Hoffman Lode parameter L^H = –0.731 had been predicted in corresponding numerical simulations [6]. For comparison, the unit cell is loaded by the load ratio $F_x/F_y/F_z$ = 1/0/0 leading to the same stress parameters η^H and L^H. The formation of the principal values of the damage strain tensor $A^{da}_{(i)}$ (20) versus the equivalent strain measure (24) is shown in Fig. 2. In particular, A^{da}_x increases up to 0.035 whereas A^{da}_y and A^{da}_z show a small decrease up to –0.006 and –0.01, respectively. This behavior is nearly identical for the different loading directions with respect to the rolling direction. In addition, the formation of the void volume fraction f (22) is shown in Fig. 3. Nearly identical behavior can be seen for the loading directions 0° and 90°

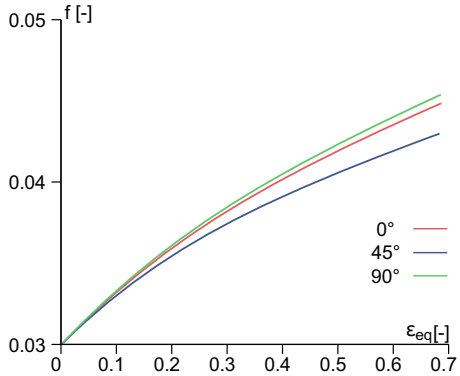

Fig. 3 Formation of the void volume fraction for $\eta^H = 0.389$ and $L^H = -0.731$

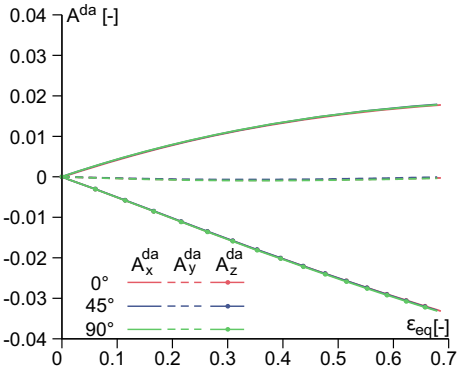

Fig. 4 Formation of principal components of the damage strain tensor for $\eta^H = 0.0$ and $L^H = 0.0$

with maximum values of 0.0415 whereas for loading direction 45° the porosity only reaches 0.040. This damage behavior was also visible in the pictures of scanning electron microscopy in [6] where large pores occur for loading in rolling (0°) and in transverse (90°) direction and less and smaller voids were visible after loading in a diagonal direction (45°). These damage mechanisms on the micro-level correspond to the slightly smaller macroscopic damage strain components and the smaller void volume fraction f numerically predicted for the diagonal direction.

For the biaxial experiments with the load ratio $F_1/F_2 = 1/-1$, the Hoffman stress triaxiality $\eta^H = 0.0$ and the Hoffman Lode parameter $L^H = 0.0$ had been predicted in corresponding numerical simulations [6]. These stress parameters have also been achieved in the unit cell calculations with the load ratio $F_x/F_y/F_z = 1/0/-1$. The evolution of the principal values of the damage strain tensor $A^{da}_{(i)}$ (20) versus the equivalent strain measure (24) is shown in Fig. 4. In this shear loading case, the damage strain component A^{da}_x increases up to 0.017 and A^{da}_z shows a decrease up to –0.032 whereas the component A^{da}_y remains 0.0. This means that during shear loading the initially spherical void is deformed into an ellipsoid. The void volume fraction f shown in Fig. 5 only shows a slight decrease of the initial void. In both

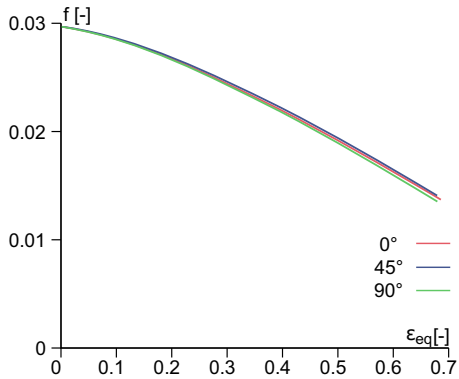

Fig. 5 Formation of the void volume fraction for $\eta^H = 0.0$ and $L^H = 0.0$

figures, nearly no effect of the loading direction on the macroscopic strain behavior can be seen. This damage behavior had also been seen in the pictures of scanning electron microscopy published in [6]. The photos showed predominant shear mechanisms on the micro-scale with only a few initial voids which were remarkably deformed in shear direction. These damage processes on the micro-scale correspond to the numerically predicted macroscopic principal damage strain components and the void volume fraction representing shear mechanisms on the macro-level with slight compression (decrease in the void volume fraction).

5 Conclusions

In the present paper, the effect of the stress state and the loading with respect to the rolling direction on damage and failure of the aluminum alloy EN AW-2017A has been examined. The results of two load cases corresponding to biaxial loading scenarios of the X0-specimen have been discussed. The stress state was characterized by the generalized stress triaxiality and the generalized Lode parameter expressed in terms of stress invariants based on the Hoffman yield criterion for anisotropic materials. Elastic-plastic constitutive parameters for the investigated ductile metal were taken from experiments performed with specimens cut from sheets in different directions with respect to the rolling direction. These parameters were used in numerical calculations considering void-containing representative volume elements. Different three-dimensional load ratios have been taken into account. Numerically predicted formations of the principal components of the damage strain tensor and of the void volume fraction as well as the corresponding damage and failure mechanisms on the micro-level have been discussed. These numerical results have been qualitatively compared with pictures from scanning electron microscopy published in the literature. The numerically predicted formation of damage strains can be seen as quasi-experimental results. They can be used to develop laws for the damage strain rates which will be taken into account in numerical simulation of experiments which will be used to validate the proposed rules for the damage strain rates with stress state and loading direction dependencies. This will be discussed in a forthcoming paper. Furthermore, the validated laws can then be used to numerically predict the deformation and failure behavior of structural components built with anisotropic sheet metals.

Acknowledgements Financial support from the Deutsche Forschungsgemeinschaft (DFG, German Research Foundation) under project number 394286626 is gratefully acknowledged.

References

1. Barsoum I, Faleskog J (2011) Micromechanical analysis on the influence of the Lode parameter on void growth and coalescence. Int J Solids Struct 48:925–938
2. Barlat F, Aretz H, Yoon JW, Karabin ME, Brem JC, Dick RE (2005) Linear transformation-based anisotropic yield functions. Int J Plast 21:1009–1039
3. Brünig M (2003) An anisotropic ductile damage model based on irreversible thermodynamics. Int J Plast 19:1679–1713
4. Brünig M (2016) A thermodynamically consistent continuum damage model taking into account the ideas of CL Chow. Int J Damage Mech 25:1130–1143
5. Brünig M, Gerke S, Hagenbrock V (2013) Micro-mechanical studies on the effect of the stress triaxiality and the Lode parameter on ductile damage. Int J Plast 50:49–65
6. Brünig M, Gerke S, Koirala S (2021) Biaxial experiments and numerical analysis on stress-state-dependent damage and failure behavior of the anisotropic aluminum alloy EN AW-2017A. Metals 11:1214
7. Brünig M, Hagenbrock V, Gerke S (2018) Macroscopic damage laws based on analysis of microscopic unit cells. ZAMM - Zeitschrift für Angewandte Mathematik und Mechanik 98:181–194
8. Brünig M, Koirala S, Gerke S (2022) Analysis of damage and failure in anisotropic ductile metals based on biaxial experiments with the H-specimen. Exp Mech 62:183–197
9. Brünig M, Koirala S, Gerke S (2023) A stress-state-dependent damage criterion for metals with plastic anisotropy. Int J Damage Mech (in press)
10. Gao X, Wang T, Kim J (2005) On ductile fracture initiation toughness: effects of void volume fraction, void shape and void distribution. Int J Solids Struct 42:5097–5117
11. Gao X, Zhang G, Roe C (2010) A study on the effect of the stress state on ductile fracture. Int J Damage Mech 19:75–94
12. Ha J, Baral M, Korkolis Y (2018) Plastic anisotropy and ductile fracture of bake-hardened AA6013 aluminum sheet. Int J Solids Struct 155:123–139
13. Hill R (1948) A theory of the yielding and plastic flow of anisotropic metals. Proc R Soc Lond 193:281–297
14. Hoffman O (1967) The brittle strength of orthotropic materials. J Compos Mater 1:200–206
15. Hu Q, Yoon JW, Manopulo N, Hora P (2021) A coupled yield criterion for anisotropic hardening with analytical description under associated flow rule: modeling and validation. Int J Plast 136:102882
16. Kim J, Gao X, Srivatsan T (2003) Modeling of crack growth in ductile solids: a three-dimensional analysis. Int J Solids Struct 40:7357–7374
17. Kuna M, Sun D (1996) Three-dimensional cell model analyses of void growth in ductile materials. Int J Fract 81:235–258
18. Scheyvaerts F, Onck P, Tekoglu C, Pardoen T (2011) The growth and coalescence of ellipsoidal voids in plane strain under combined shear and tension. J Mech Phys Solids 59:373–397
19. Stoughton TB, Yoon JW (2009) Anisotropic hardening and non-associated flow rule in proportional loading of sheet metals. Int J Plast 25:1777–1817
20. Tsutamori H, Amaishi T, Chorman RR, Eder M, Vitzthum S, Volk W (2020) Evaluation of prediction accuracy for anisotropic yield functions using cruciform hole expansion test. J Manuf Mater Process 4:43